Macromolecules

Volume 25, Number 23 November 9, 1992

Structure/Properties of Conjugated Conductive Polymers. 1. Neutral Poly(3-alkylthiophene)s

Show-An Chen* and Jui-Ming Ni

Chemical Engineering Department, National Tsing-Hua University, Hsinchu, Taiwan 30043, China

Received July 1, 1991; Revised Manuscript Received June 30, 1992

ABSTRACT: Soluble conjugated poly(3-alkylthiophene)s (P3ATs) including poly(3-butylthiophene) (P3BT), poly(3-octylthiophene) (P3OT), and poly(3-dodecylthiophene) (P3DDT), were prepared chemically and characterized by use of various thermal analysis and spectroscopic methods and conductivity measurement. It is found that each of the P3ATs consists of an ordered phase and a disordered phase. In the ordered phase, the side chains are nearly fully extended and are packed to give a two-layer structure and one-layer structure, the former being the majority. The coplanar subchains are stacked to form planes, and the space between two successive stacking planes is filled with aligned side chains. For the longer side chain such as in P3DDT, the ordered side chains also form a separated ordered phase. As the ordered phase melts, a thermochromism occurs. In the disordered phase, three transitions are observed, being γ, β, and α resulting from relaxations of methylene linkages, side chains, and twists in the main chains (noncoplanar segments or conformons), respectively. The γ and β relaxations provide only a slight disturbance to the coplanarity in the main chains. However, the α relaxation has a significant effect on the optical band gap by an increase of the distortion in the soft conformons (in which the torsion between two coplanar subchains is distributed over several repeated units), leading to a localization of their π electrons and therefore a hindrance to the intrachain (and perhaps interchain) charge transport. As temperature increases to about 30–60 °C above T_α, the hindrance effect on charge transport is dominated over the increased charge mobility, causing an occurrence of conductivity maximum. This conductivity maximum can be considered as another characteristic of the electronic structure of the π system in addition to the thermochromism at the melting temperature of the ordered phase.

Introduction

Polythiophene (PT) is an environmentally stable conjugated polymer in both neutral form and doped form having a conductivity as high as 500 S/cm[1] and thus has been extensively investigated. Introducing a flexible side chain such as an alkyl group with a carbon number of 4 or more on the 3-position of the thiophene ring allows the polymer to be soluble in common organic solvents, fusible, and melt processable yet retains a rather high conductivity of about 30–100 S/cm.[2-4] Experimental and theoretical studies of poly(3-alkylthiophene)s (P3ATs) on their structures and thermo- and solvatochromisms have been extensive.

A poly(3-hexylthiophene) (P3HT) solution in chloroform, on addition of the nonsolvent acetonitrile, can shift from yellow to magenta (solvato chromism) as a result of a rod-to-coil transition of the molecular chains.[4] Upon heating a P3HT film from room temperature up to 240 °C, a blue shift of the optical absorption peak was observed, which was attributed to a reduction of the conjugating length. Upon cooling, this peak red-shifted toward its initial value (thermochromism).[5] X-ray diffraction profiles at room temperature for P3AT indicates a presence of the disordered structure and ordered structure with low crystallinity.[5,6] The presence of a multiphase was also suggested based on the disappearance of the second shoulder at 2.21 eV before the first at 2.04 eV in the optical spectrum upon heating and on the absence of an isosbestic point in the optical absorption spectra at various temperatures.[7,8]

The thermochromism and solvatochromism were also considered on a molecular level as a result of the interruption of conjugation caused by a generation of twists (disruption of planarity).[7,9] These twists, which were termed "conformons", partition a polymer chain into subchains having a distribution of smaller conjugating length as evidenced by the continuous shift of optical absorption maximum with increasing temperature or solvent power. The density of conformons is increased at a higher temperature or solvent power. It was proposed that a creation of conformons close to existing conformons could be easier than a creation of new conformons, since extra energy is required for the rotation due to interaction with the neighboring polymer molecules. Three cases of the rotational defects (or conformons) were proposed, being

* Author to whom correspondence should be addressed.

0024-9297/92/2225-6081$03.00/0

(i) a localized conformon (twist), where the twist occurs between two repeating units previously in the plane with their neighbors of the same chain; (ii) a soft conformon, where the torsion between the two coplanar subchains is distributed over several repeating units; and (iii) wormlike chains (which appear at high temperature), in which no repeating unit is in the plane with its neighbors of the same chain.

These conformational defects which lead to a chromism were further elucidated by use of XPS and UPS (ultraviolet photoelectron spectroscopy) examinations on P3HT in light of valence effective Hamiltonian (VEH) quantum mechanical calculations starting from the fully planar anti form.[9-11] The conjugating length or number of coplanar rings at low temperature (-60 °C) is about or greater than 7, at room temperature is about 4.5, and at high temperature (above 190 °C) is between 2 and 3. The increased thermal motion of the alkyl side chain is intimately involved in the thermochromic effect by influencing the planarity of the backbone of polymer chains and therefore the electronic structure. Optical spectroscopic examination of the effect of side-chain length on the electronic structure of the P3ATs indicates that the temperature at which thermochromism occurs decreases with an increase in the length of the alkyl side chain with carbon numbers of 4-10. This temperature is rather close to the melting temperature observed by use of thermal analysis.[8]

From the reviews above, it is known that thermochromism and solvatochromism of P3ATs result from the disruption of the planarity of the subchains due to the presence of alkyl side chains, since no thermochromism was observed in PT. However, alignment and packing of the polymer chains as well as the extent of thermal motion of the conformons and alkyl side chains at various temperature levels and their effects on the electronic structure of the π system have not been well clarified. In this work, these factors are studied by use of thermal analysis (dynamic mechanical analysis and differential scanning calorimetry), spectroscopic analysis (UV-vis and X-ray diffraction), and measurement of the conductivity variation with temperature. The polythiophenes investigated involved polythiophene (PT), poly(3-methylthiophene) (P3MeT), poly(3-butylthiophene) (P3BT), poly(3-octylthiophene) (P3OT), and poly(3-dodecylthiophene) (P3DDT).

Experimental Section

1. Synthesis of Polymers and Preparation of Samples. Neutral P3ATs were prepared following the chemical method used by Sugimoto et al.[12] A 0.1 N 3-alkylthiophene monomer was oxidation-polymerized in a 0.4 N $FeCl_3$ solution in chloroform at room temperature under a nitrogen atmosphere. The resulting mixture was then poured into methanol to precipitate out the polymer. This polymer was then washed several times with methanol and then extracted with methanol in a Soxhlet extractor in order to remove the residual oxidant and oligomers. The purified polymer (except P3MeT) was then dissolved in chloroform. The resulting solution was filtered in order to remove insoluble gels. Then the clear solution was cast in a Teflon mold to give a film with a thickness of about 0.1 mm. This thin film, after dynamic vacuum pumping until a constant weight was retained, was ready for physical characterizations.

A neutral polythiophene (PT) film was prepared following the electrochemical method used by Hotta et al.[13]

2. Characterizations. Gel permeation chromatography (Waters Model 201) with a UV detector at 400 nm and a column of Ultrastyragel linear P/N 10681 from Waters was used to measure the molecular weight distribution (MWD) relative to polystyrene standards. The calibration curve was determined by use of 10 MW standards from MW 2000 to 10^6. The carrier solvent used was tetrahydrofuran at a flow rate of 1 mL/min.

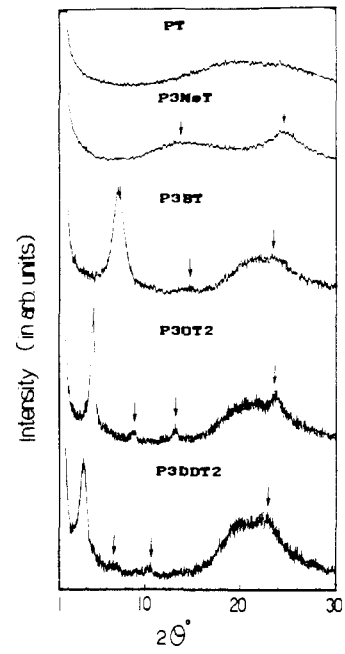

Figure 1. X-ray diffraction patterns of the pure PT, P3MeT, and P3ATs.

X-ray diffractions were measured using a Rigaku Model D/Max-2B diffractometer. The X-ray beam was nickel-filtered Cu Kα (λ = 0.1506 nm) radiation from a sealed tube operated at 30 kV and 20 mA. Data were obtained from 1° to 45° (2θ) at a scan rate of 1°/min with a smoothing number of 7.

A dynamic mechanical analyzer (Du Pont Model DMA983) was used to measure the dynamic moduli (E' and E'') and loss tangent (tan δ) of the polymer films in the temperature range -150 to +200 °C at a heating rate of 2 °C/min and a frequency of 1 Hz. The sample size was about 10 mm long, 2 mm wide, and 0.1 mm thick. After mounting in the sample chamber, the sample length subject to cyclic flexual motion was about 1 mm.

A differential scanning calorimeter (DSC; Du Pont Model DSC10) was used to examine thermograms in the temperature range -100 to +300 °C with a heating rate of 10 °C/min. The temperature at a melting peak was taken as the melting temperature, while the glass transition temperature was taken at the maximum of the first-order derivative of the thermogram. Thermograms of a second run were obtained by cooling the sample from a first run to room temperature and then following the procedure for the first run. Cooling scans were also performed by use of DSC (Perkin-Elmer Model DSC-2C) at a cooling rate of 10 °C/min.

Ultraviolet-visible spectra (UV-vis) at -100 to +250 °C were recorded using an UV-vis spectrophotometer (Shimatzu Model UV-160). The spectrophotometer was equipped with a variable-temperature cell to allow for measurement of spectra under vacuum from -100 to +250 °C; the soaking time was 10 min at each specific temperature, and the heating rate used was about 1-2 °C/min during heating. The testing sample was prepared by coating a P3AT solution in chloroform on a piece of quartz and allowing it to dry to give a coated film with a thickness on the order of 1 μm.

Conductivities of the neutral P3ATs and PT along the film thickness direction were measured using the two-disk method[14] under dry nitrogen purging from 0 to 300 °C at a heating rate of about 2 °C/min.

Results and Discussion

1. Gel Permeation Chromatography (GPC) Results. The number- and weight-average molecular weights, $\bar{M}_n$ and $\bar{M}_w$, and average degree of polymerization $\overline{DP}_n$ (relative to the molecular weight standards of polystyrene) of the P3ATs so obtained are listed in Table I. The $\bar{M}_w$s are on the order of 10^5, which is sufficiently high to be considered as a high polymer. The MWDs are rather

Table I
Average Molecular Weights of P3ATs Relative to Polystyrene Standards

	polymn time (h)	$\bar{M}_n \times 10^4$	$\bar{M}_w \times 10^5$	$\bar{M}_w/\bar{M}_n$	$\overline{DP}_n$
P3BT	10	2.6	1.5	5.9	188
P3OT1	10	2.1	1.1	5.2	108
P3OT2	24	4.8	2.4	5.1	247
P3DDT1	10	2.0	1.1	5.6	80
P3DDT2	24	5.1	2.6	5.1	204

Table II
X-ray Diffraction Maxima and Calculated *d* Spacing of the Pure PT, P3MeT, and P3ATs

	2θ (deg)/*d* spacing (Å)				calcd values[a] of *d* spacing:
	small angle			wide angle	
	first	second	third		first
PT				pr[b]	
P3MeT	14.0/6.0			24.6/3.6	
P3BT	7.1/12.4	14.3/6.2		23.3/3.8	13.1
P3HT[c]	5.3/16.8	10.6/8.4	15.9/5.6	23.4/3.8	17.4
P3OT2	4.6/19.4	8.8/10.1	13.1/6.7	23.6/3.8	21.7
P3DDT2	3.5/25.1	6.7/13.2	10.6/8.3	22.9/3.9	30.4

[a] Calculated from the ideal model proposed by Thémans et al.,[11] in which the side chain is fully extended and forms an angle of 31.8° with the vertical axis in the plane of the thiophene ring and the main chain has a transoid conformation. [b] pr means poor resolution. [c] Taken from ref 5.

broad, having a low MW tail and a polydispersity of about 5. However, only a single-mode MWD for each P3AT was observed. For P3OT and P3DDT, samples of two different MWs (varying by a factor of about 2.3) were prepared and denoted as "1" and "2" for lower and higher MWs, respectively.

2. X-ray Diffractions. X-ray diffraction patterns of P3ATs, P3MeT, and PT are shown in Figure 1, and their characteristic angles at intensity maxima and corresponding values of *d* spacings calculated using Bragg's law are listed in Table II.

For PT, only a very broad single diffused scattering peak with a maximal intensity at about 20° is observed, indicating that no crystallinity can be observed by the X-ray diffraction and that there exists a broad distribution of intraplanar and interplanar distances.[15] For P3MeT, two diffused scattering peaks are observed, one at the wide angle 24.5° and the other at the small angle 14.0°. The former can be attributed to the disordered phase and the latter to the interplanar spacing with broad distribution resulting from the presence of methyl groups as in the case of the comblike polymers poly(*n*-alkyl acrylate)s, with a carbon number of the alkyl group from 1 to 4.[15] For P3ATs, in addition to the amorphous peak at wide angle, a peak with moderate to weak intensity also appears at the wide angle. The corresponding values of *d* spacing are rather close, being 3.9, 3.8, and 3.8 Å for P3DDT2, P3OT2, and P3BT, respectively. For P3HT, there is also a diffraction peak at wide angle corresponding to a *d* spacing of 3.8 Å; this side-chain-length-independent *d* spacing, 3.8 Å, can be attributed to the spacing between two successive stacking planes of coplanar subchains (or intraplanar spacing) as was also assigned for P3HT.[5] Furthermore, at low angle, three diffraction peaks for P3OT2 and P3DDT2 and two diffraction peaks for P3BT are observed. On examination of the first-order reflection, the corresponding *d* spacings are found to increase with an increase in the length of the alkyl side chain (*d* = 12.4 Å for butyl and 25.1 Å for dodecyl); the same also appears for the second- and third-order reflections. Hence, these reflections must indicate that the space between two

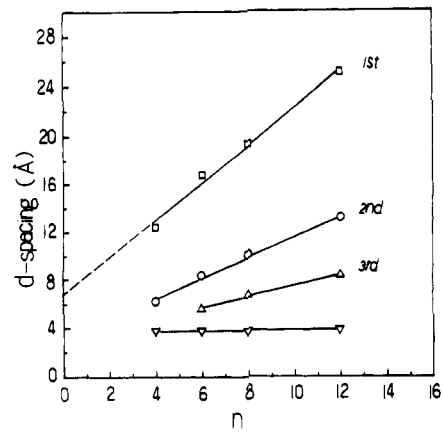

Figure 2. Plots of the *d* spacing from X-ray reflections versus the number of carbon atoms in the side chains.

neighboring coplanar subchains on the same plane must be filled with the side chains. The presence of the second- and third-order reflections indicates a higher degree of space filling of the alkyl side chains. The same situation also occurs for the comblike polymers with alkyl side chains such as poly(*n*-alkyl acrylate)s, poly(*N*-alkylacrylamide)s, etc.[16,17]

Plots of the values of the *d* spacing of the first three diffraction peaks at low angle and the diffraction peak at wide angle versus the number of carbons of the side chains of P3ATs give four straight lines as shown in Figure 2. For the *d* spacing corresponding to the first-order reflection, the calculated value for each P3AT is based on two-layer packing with two neighboring side chains (all-trans conformation) on the same side-chain axis of two neighboring coplanar subchains laying on the same plane (see Figure 8a in the later section). It is obtained by summing the diameter of a thiophene ring, 2.5 Å (estimated from the geometric structure of thiophene[11]) and twice the sum of the lengths of one ring–C bond (1.54 Å), $m-1$ times the C–C bond length projected on the axis of the extended side chain (1.27 Å), and one terminal C–H bond projected on the same axis (1.1 A) and then multiplying by cos (31.8°) (or 0.85). Here m is the carbon number of the alkyl group and 31.8° is the angle between the axis of the extended side chain and the vertical axis on the same plane of the ring, as estimated from the geometric structure of the antiform of P3AT proposed by Thémans et al.[11] using MNDO calculation. The calculated values are remarkbly close to the experimental values of the *d* spacing and deviate by +0.7, +0.6, +2.3, and +5.3 Å for P3ATs with alkyl side chains of m = 4, 6, 8, and 12, respectively; only m = 12 has a higher deviation, indicating that side-chain torsion and/or partial intercalation might occur for P3DDT. For the *d* spacing corresponding to the second-order reflection, its value is almost exactly half that of the *d* spacing corresponding to the first-order reflection. This indicates an existence of one-layer packing, which could probably be formed by intercalation of the extended (or torsional for m = 12) side chains between two neighboring coplanar subchains (see Figure 8b in the later section). The one- and two-layer packings (interplanar packing) must also accompany a presence of intraplanar stacking (as is just the case due to the presence of the diffration peak at 22–24°) so that stability of the packing can be maintained. Evidently, the two- and one-layer packings do exist in the supermolecular structure of P3ATs; the fraction of the former is much higher than that of the latter, as can be inferred from the much higher diffraction intensity of the first-order reflection than the second-order reflection. The origin of the third-order reflection could

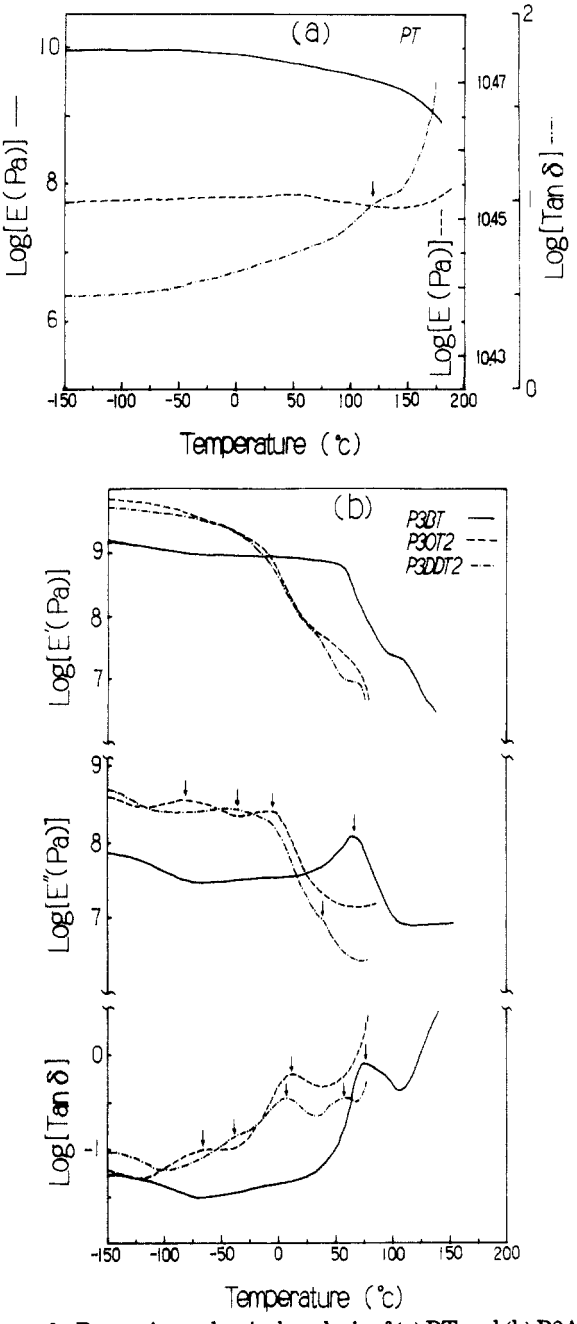

Figure 3. Dynamic mechanical analysis of (a) PT and (b) P3ATs at a frequency of 1 Hz and a heating rate of 2 °C/min.

be attributed to a one-layer packing with more conformational freedom of the side chains; the fraction of the polymer with this structure is also very small. The straight line plot in Figure 2 also appears for poly[10-[(*n*-alkylhydroxy)carbonyl]-*n*-decylmaleimides] with the carbon number of the alkyl group (an even number) being 2–22.[18] The geometric structure of this series of polymers is very similar to the P3ATs; the repeating unit is also composed of a five-membered ring and a linear side chain.

3. Dynamic Mechanical Analysis (DMA). DMA of PT and P3ATs are shown in parts a and b of Figure 3, respectively. The characteristic temperatures of tan δ and loss tensile modulus E'' maxima are listed in Table III. As can be seen, each P3AT exhibits three transitions, being γ, β, and α resulting from relaxations of methylene linkages, side chains, and twists (disordered segments or conformons) in the main chains, respectively, as demonstrated below. The γ transitions of the P3ATs all have a peak with significant size at a temperature below −150 °C and can be assigned as a relaxation of methylene linkages of

Table III
Transition Temperatures (°C) of the Pure PT and P3ATs from Dynamic Mechanical Analysis

	peak temp (°C)							
	γ		β		α		T_s[a]	
	tan δ	E''	tan δ	E''	tan δ	E''	tan δ	E''
PT					120			
P3BT	<−150	<−150	nc[b]	nc	75.4	65.7		
P3OT2	<−150	<−150	−66.6	−80.3	11.2	−6.4		
P3DDT2	<−150	<−150	−37.4	−37.3	5.6	pr[c]	57.4	nc

[a] T_s = melting temperature of ordered side chains. [b] nc means "not clear". [c] pr means "poor resolution".

the side chains. The reasons are as follows: PT has no such relaxation in the vicinity of this temperature (as shown in Figure 3a) and the relaxation of the methylene linkages in polyethers usually occurs at about −130 °C[19] and in comblike structure polymers with an alkyl side chain (e.g., poly(*n*-alkyl methacrylate)s) below −150 °C.[20] For the α transition, the elastic tensile modulus E' drops by a factor of 10^2, which is the same as that in the glass transition of conventional amorphous or partially crystalline polymers. Thus, the α relaxation can be regarded as the glass transition of the disordered phase, while the β transition lying in between the γ and α transitions must be due to a relaxation of the side chains.

For P3OT2, the β relaxation appears as a rather flat peak at −66.6 °C, which is immediately followed with the α relaxation, indicating that the relaxation of the conformons in the main chains is induced by the increased thermal motion of the alkyl side chains.

For P3DDT2, the β relaxation peak is present as a shoulder and is followed immediately by the α relaxation peak, indicating that the α transition starts before the completion of the β transition. In other words, the effect of the thermal motion of the side chains on the thermal motion of the conformons is higher than that of P3OT due to the longer side chain. The T_β (−37.4 °C) is higher than that of P3OT (−66.6 °C). This is reasonable, since the relaxation of the longer alkyl side chain would require a higher thermal energy and therefore occur at a higher temperature as in the case of comblike structure polymers with alkyl side chains.[21] The T_α (5.6 °C) is lower than that of P3OT (11.2 °C), which can be attributed to the higher free volume provided by a plasticization effect of the longer alkyl side chains in the disordered phase, since at that temperature the side chains are already relaxed. As the temperature further increases, the tan δ curve shows a maximum at 57.4 °C, which can be assigned as the melting temperature of the ordered alkyl side chains in the ordered phase, since the E' in the vicinity of this temperature is present as a plateau.

For P3BT, the β transition seems to occur from about −75 to 20 °C and has no observable peak, indicating that thermal motion of the shorter side chain is coupled with thermal motion of the attached thiophene ring. The α transition peak is centered at 75.4 °C, higher than the estimated value from extrapolation of the T_αs of P3OT2 and P3DDT2 by about 20 °C. In addition, in the glassy region, tan δ is lower than those of P3OT2 and P3DDT2, reflecting a lower extent of the relaxation effect during this temperature range, while E' in this temperature period remains at a rather constant level. These results imply that the β transition probably does not occur.

Dynamic viscoelasticities of conjugated polymers (in free-standing film form) were first measured for *cis*- and *trans*-polyacetylenes (PAs) by one of us in order to investigate the behaviors of cis–trans isomerization and

oxidation when exposed to air.[22,23] It was found that T_g was not observed between −100 to +150 °C and can be expected, if there is one, to be greater than 200 °C, as can be estimated from the results of the small tan δ value at 150 °C (0.01–0.02)[22] and T_gs of alkyl-substituted PAs measured by Higashimura and co-workers.[24] As in the present P3ATs, for the substituted PAs, an increase of the length of the alkyl side chain can cause a reduction of T_g. However, the side-chain effects on the coplanarity of the repeating units are dramatically different. As the length of the alkyl side chain increases, for the neutral P3ATs, the average conjugating length also increases, as reflected in the decreased energy of the absorption maximum (see later section), while for the neutral substituted PA, the intrinsic conductivity decreases[25] (reflecting a decreased coplanarity).

4. Differential Scanning Calorimetry (DSC). DSC thermograms of PT and P3ATs are shown in Figure 4, and their characteristic values (glass transition temperature T_g, melting temperature and heat of melting of the side chains T_s and ΔH_s, and melting temperature and heat of melting of the main chains T_m and ΔH_m) are listed in Table IV. T_g and T_s were assigned by assistance of the DMA results.

For P3BT, two endothermic peaks are observed in the first heating run, one at 64.9 °C and the other at 229.2 °C; the former transition can also be characterized by the temperature of maximum rate of heat flow, 58.7 °C. In the second heating run, the first peak becomes a step drop as for the normal glass transition of conventional polymers and can be characterized by 50.2 °C (at which the rate of heat flow is maximum), and the second peak disappears. Since the transition temperature at 58.7 °C from DSC is close to the T_α (75.4 °C) obtained from DMA, it can be assigned as the glass transition temperature T_g. The second peak can be attributed to the decomposition of the dopant, since this peak also appears in the $FeCl_3$-doped P3BT (see Figure 4a) and in $FeCl_3$-doped P3HT as observed by the others.[26] In the cooling scan (Figure 4b), the P3BT thermogram shows no exothermic peak below 250 °C. Thus it can be considered that P3BT has no observable melting peak below 300 °C, but it does contain some subchains aligned in ordered fashion as reflected in the results of X-ray diffraction and UV–vis spectroscopy (see later section).

For P3OT1, the DSC thermogram of the heating scan shows the T_g at −11.3 °C and the T_m at 133.5 °C. As the MW is increased (P3OT2), the T_g (−7.0 °C) increases slightly by 4.3 °C, and T_m (150.0 °C) and ΔH_m increase significantly by 16.5 °C and 22%, respectively. These would indicate that the chain end defect can lead to a decrease of ordering in both the ordered and disordered regions. In the second run, for P3OT2, T_g drops by 7.2 °C and T_m by 2.6 °C, but ΔH_m increases by 2 J/g or 55%. In the cooling scans, both higher and lower MW P3OT show exothermic peaks at 78.6 and 62.1 °C, respectively. This result further confirms that P3OT has an ordered phase, of which the fraction increases with increasing MW. In comparison to P3BT, the presence of an ordered phase in P3OT2 indicates that the longer alkyl side chain can provide a higher free volume, allowing the molecular chains to realign more easily than the shorter alkyl side chain.

For P3DDT2, in addition to the presence of T_g (−18.5 °C) and T_m (116.3 °C), an endothermic peak (at 56.1 °C) in advance of the melting peak is observed in the thermogram of the heating scan, of which the endothermic heat is much higher than ΔH_m by a factor of 1.7. The thermogram of the second run also shows the presence of this peak in addition of the melting peak. In conjunction with the presence of a transition centered at 57.4 °C, which is 51.8 °C higher than T_α in the tan δ curve, and the presence of the second plateaus in the range of 50–70 °C in the E' curve of DMA, this peak can be attributed to a melting of the ordered side chains. This melting peak for ordered side chains is immediately ahead of the melting peak for the ordered subchains, reflecting that the ordered subchains always accompany ordered side chains and that

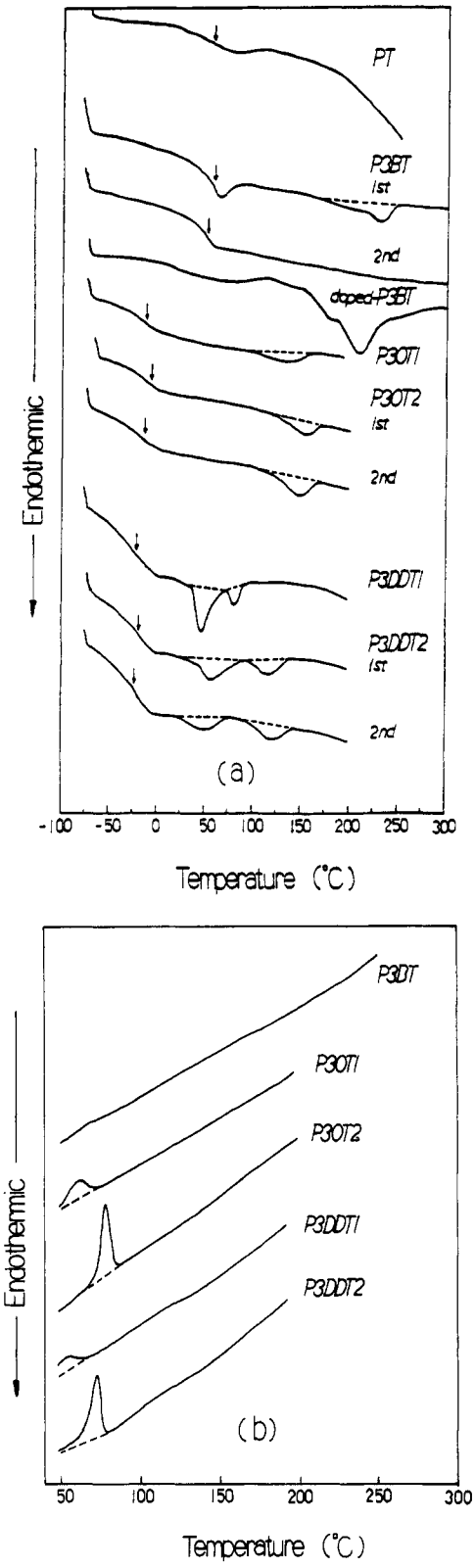

Figure 4. DSC thermograms: (a) PT, P3MeT, and P3ATs in the heating scans at a heating rate of 10 °C/min. For the doped P3BT the scale is amplified by a factor of 2. (b) P3ATs in the cooling scans at a cooling rate of 10 °C/min.

Table IV
Thermal Properties of PT and P3ATs from DSC

	T_g (°C)		T_s (°C)		T_m (°C)		ΔH_s (J/g)		ΔH_m (J/g)	
	1st run	2nd run	1st run	2nd run	1st run	2nd run	1st run	2nd run	1st run	2nd run
PT	58.7									
P3BT	58.7	50.2								
P3OT1	−11.3	nm[a]			133.5	nm			2.9	nm
P3OT2	−7.0	−14.2			149.9	147.3			3.6	5.6
P3DDT1	−20.0	nm	47.3	nm	81.1	nm	7.2		1.8	nm
P3DDT2	−18.5	−22.1	56.1	51.8	116.3	119.3	6.1	3.9	3.6	4.2

[a] nm means "not measured".

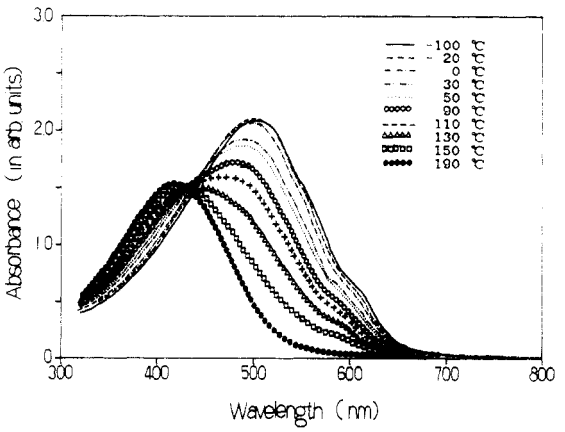

Figure 5. UV–vis absorption spectra of a P3OT1 film at various temperatures from −100 to +190 °C.

even when the ordered side chains are melted, the ordered main chains can still retain their ordered packing arrangement. The phenomenon of separate meltings of ordered side chains and main chains also occurs in comblike structure polymers, such as poly(1-alkylethylene)s,[27] in which the side chains also participate in the formation of a crystalline phase together with the main chains where the length of the side chain reaches 10–12 carbons as in the case of the P3DDT. As the MW decreases (P3DDT1), the T_g, T_s, and T_m decrease by 1.5, 8.8, and 35.1 °C respectively. Such drops of the characteristic temperatures can be attributed to a decrease of the ordering in both the ordered and disordered regions resulting from the increase in chain end defects. In the cooling scans from 250 to 50 °C, both higher and lower MW P3DDT show exothermic peaks at 72.1 and 55.0 °C, respectively (Figure 4b), confirming the presence of an ordered phase.

In comparison of T_g with T_β and T_α from the results of DMA of P3ATs, for P3OT and P3DDT, T_g locates in between T_β and T_α, indicating that T_g from DSC could result from the relaxation of disordered subchains and side chains, but, for P3BT, T_g (58.7 °C) is more close to T_α (75.4 °C); this result also supports that the relaxations of the conformons and disordered side chains are coupled.

For PT, the DSC thermogram (on the top of Figure 4a) shows a transition centered at 58.7 °C, which can be attributed to a relaxation of conformons. This transition temperature seems too low to be taken as T_g for a linear PT with α,α'-coupling, which would be higher than 58.7 °C as can be inferred from the T_gs of P3AT in Table IV. Such low T_gs must be due to structure defects such as cross-linking and α,β-coupling for thiophene rings, which usually appear in PT and P3MeT films with a thickness greater than 1 μm (in the present case, 10 μm) prepared using the electrochemical method.[28,29]

5. Ultraviolet–Visible Spectroscopy (UV–vis). UV–vis spectra of the P3ATs at −100 to +250 °C were measured, and only those of P3OT1 are presented in Figure 5 because of their similarity. The spectra from 190 to 250 °C are

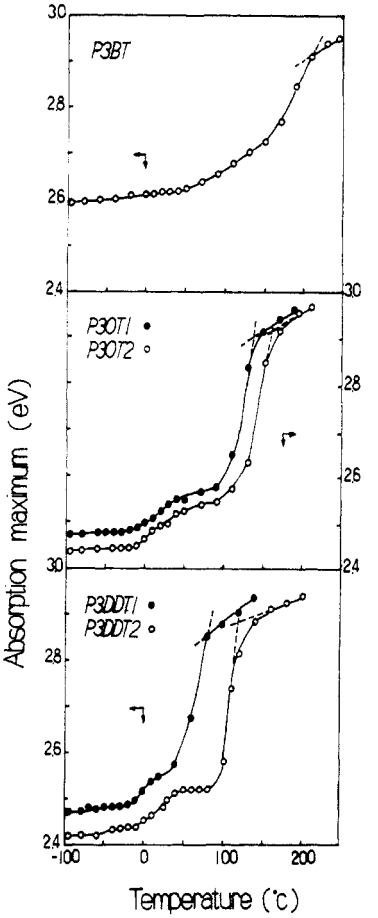

Figure 6. Plots of the energy of absorption maximum in the UV–vis spectra versus temperature for thin films of P3ATs.

about the same, except a slight increase in energy of the absorption maximum; thus only the spectrum at 190 °C is shown. Plots of the energy of absorption maximum versus temperature of the spectra of the P3ATs are shown in Figure 6. Since the energy of absorption maximum is a measurement of the energy for a π–π^* transition, it is represented here in the units of energy eV. In Figure 6, the absorption maximum curves can be divided into several stages as shown in Table V. In Table V, the temperature ranges of various transitions determined from the thermal analysis (DMA and DSC) are also included for comparison. The temperature range of each stage determined from the UV–vis result is in agreement with that determined from the thermal analysis.

For P3DDT2 (high MW), as can be seen from Figure 6 and Table V, the β relaxation (stage 1, −100 to −40 °C) has a slight effect on the coplanarity of thiophene rings upon an increase of the energy by 0.017 eV, while α relaxation (or relaxation of conformons) in the disordered region (stage 2, −40 to +40 °C) can result in an increase of the energy of absorption maximum significantly. In this period, the conjugating length or band gap decreasing by

Table V
Temperature Ranges (°C) of Various Transitions Determined from DMA, DSC, and UV-Vis

	DMA[a] and DSC (°C)				UV-vis (°C)	
polymer	onset	end	method	transition	onset	end
P3DDT2	<-150	-100	DMA	γ relaxn		
	-100	-25	DMA	β relaxn	-100	-40
	-25	35	DMA	α relaxn	-40	40
	35	70	DSC	side-chain melting	40	90
	90	140	DSC	main-chain melting	90	115[b]
P3OT2	<-150	-120	DMA	γ relaxn		
	-120	-35	DMA	β relaxn	-100	-10
	-35	40	DMA	α relaxn	-10	80
	100	165	DSC	melting of main and side chains	80	160[b]
P3BT	<-150	-70	DMA	γ relaxn		
	-70	110	DMA	β and α relaxn	-100	150
				melting of main and side chains	150	200[b]

[a] tan δ curves of DMA were used in the determination of onset and end temperatures of the three relaxations. [b] See Figure 6 for the determination of the end temperature of melting, which is also regarded as the transition temperature (T_{tr}) for thermochromism.

0.083 eV is observed, indicating that the π electrons in the conformons also participate in the delocalization with the coplanar subchains, but to a lesser extent than those in the coplanar subchains. As temperature further increases to the melting region of ordered side chains (stage 3, 40–90 °C), the energy of absorption maximum has no appreciable change. This is in agreement with the DSC result that, as the ordered side chains are melted, the ordered subchains still retain their coplanarity. In the melting region of the ordered subchains, the energy of absorption maximum increases abruptly by about 0.36 eV. The entire process has an energy change of 0.46 eV. As MW drops (P3DDT1), the entire progression of the absorption maximum raises to a higher energy level, indicating a lower conjugating length at the same temperature. This lowering in conjugating length as MW decreases obviously results from the increased number of free chain ends. The entire process has an energy increase of 0.375 eV, which is smaller than that of the higher MW P3DDT by 0.085 eV.

For P3OT2 (high MW), as in the case of P3DDT, the β relaxation has little effect on the coplanarity of thiophene rings upon an increase of the energy by 0.012 eV, while the occurrence of α relaxation can result in an increase of the energy of absorption maximum significantly; from the onset temperature of the relaxation up to the onset of melting, it increases by about 0.093 eV. In the melting region of the ordered phase, the energy of absorption maximum also increases abruptly by 0.35 eV. The entire process has an energy change of 0.455 eV. As MW drops (P3OT1), the entire progression of the absorption maximum also raises to a higher energy level. The entire process has an energy increase of 0.425 eV, which is smaller than that of the higher MW P3OT by 0.031 eV.

For P3BT, the energy of absorption maximum increases concave upward and smoothly with increasing temperature; to assign the onset and end temperatures of the β and α relaxations is difficult. This observation is also in agreement with the observation of DMA that the thermal motions of the side chain and main chain are coupled. However, with the aid of DMA and DSC results (see Table V), the onset and end temperatures of β and α relaxations together can be assigned as −100 and +150 °C, respectively, during which the energy increases by 0.146 eV. For the entire process, the energy change is 0.312 eV.

In a comparison of these three P3ATs, the shift in energy of absorption maximum resulting from the α transition and melting increases with an increase in MW and the length of side chain, while, in the frozen state (at −80 °C or lower), the energy of absorption maximum decreases with an increase in MW and the length of side chain. Thus, it is likely that the presence of a side chain can promote the extent of coplanarity of the thiophene rings by providing an increased free volume to allow an alignment of the main chains into ordered aggregates more easily. Such an increase in free volume also causes the polymer to melt at lower temperature, while the decrease in the free chain ends at higher MW also provides less conjugational defect.

From the increase of the energy of absorption maximum by less than 0.1 eV during the α relaxation period, it can be inferred that, before the start of α relaxation, the conformational defect in the main chains is of soft conformon, in which the distortion is distributed over several repeating units between two successive coplanar subchains. The torsion angles between two successive rings in the frozen soft conformons would be sufficiently small to allow π electrons in the soft conformons to participate in the delocalization with their immediate neighboring coplanar subchains of the same polymer chain. During the period of α relaxation, the torsion angle increases, and the previously delocalized π electrons in the soft conformons now localized. The soft conformons gradually turn to localized conformons. After completion of the α relaxation, the coplanar subchains in the ordered phase still retain their conjugating lengths. During the melting period, the ordered phase is melted and new localized conformons are generated; the conjugating length is reduced to 2 or 3.

6. Conductivity Measurements. Conductivity versus temperature plots from 0 to 300 °C for the neutral PT and P3ATs are shown in Figure 7. As can be seen, each of the conductivity curves of P3ATs exhibits a maximum. For PT, a local maximum at 105 °C is observed; the conductivity then further increases with increasing temperature. The temperature at conductivity maximum is listed in Table VI. The occurrence of conductivity maxima during heating and cooling was also observed in neutral P3DDT and poly(3-docosylthiophene) by Yoshino et al.[30] In a measurement of charge mobility versus $1/T$ for neutral P3HT used as a semiconductor in a thin film field-effect transistor, a maximum at 72 °C was observed,[31] which is consistent with our observation of the temperatures at conductivity maxima. In both works, no satisfactory interpretations for the occurrence of the maxima of conductivity and charge mobility were given.

The temperature at conductivity maximum of P3AT decreases with an increase in the side-chain length, increases with an increase in the MW, and is higher than the T_α determined from tan δ curves of DMA by about

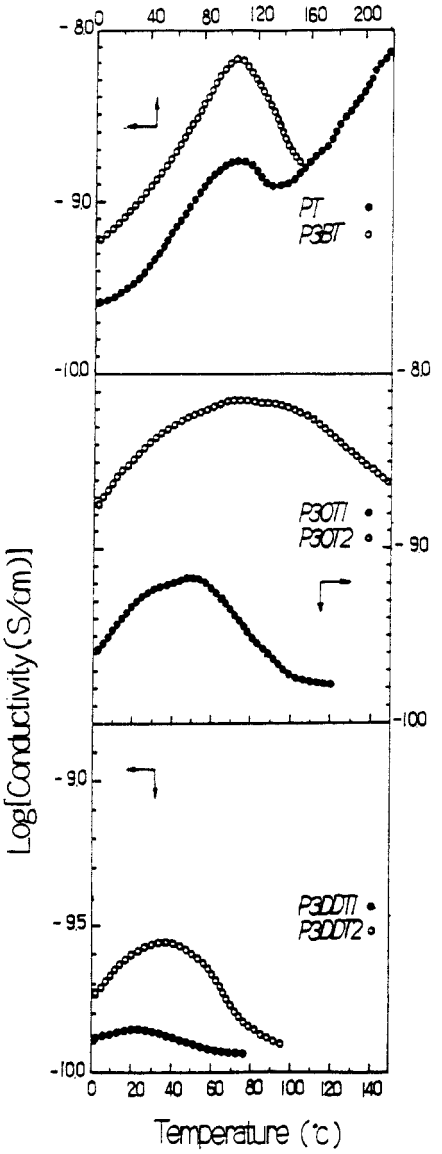

Figure 7. Conductivity versus temperature of films of PT and P3ATs.

Table VI
Temperatures at Conductivity Maxima of P3ATs (°C)

	$T_{conduct\ max}$		$T_{conduct\ max}$
PT	105[a]	P3OT2	72
P3BT	104	P3DDT1	22
P3OT1	48	P3DDT2	39

[a] After passing this local maximum, the conductivity increases with temperature again.

30–60 °C. Thus, the presence of conductivity maximum can be attributed to the occurrence of the relaxation of the conformons as illustrated below. Although the α relaxation can only cause an increase of the energy of the π–π^* transition by less than 0.1 eV, much less than that by the melting of ordered subchains, about 0.35 eV, this increased distortion of conformons would make a delocalization of their π electrons with its neighboring coplanar subchains difficult and therefore reduce the conductivity. Although the electron mobility increases with increasing temperature, it is compensated by the increased ring distortion in the conformons due to the α relaxation. These two factors compete during the relaxation period. As temperature increases the latter becomes more important than the former; the conductivity then drops. Thus the temperature at conductivity maximum is higher than T_α, as is just the case. After the completion of the α relaxation process, a further increase in the temperature leads to a melting of the ordered phases. Thus conductivity decreases with a further increase in temperature. For PT, after the occurrence of local maximum at 105 °C, the conductivity then increases with temperature. This is due to the absence of melting of the coplanar subchains below 300 °C. The occurrence of conductivity maximum can be considered as another characteristic of the electronic structure of the π system, in addition to the thermochromism, of which π electrons in the ordered phase are localized due to a loss of conjugation.

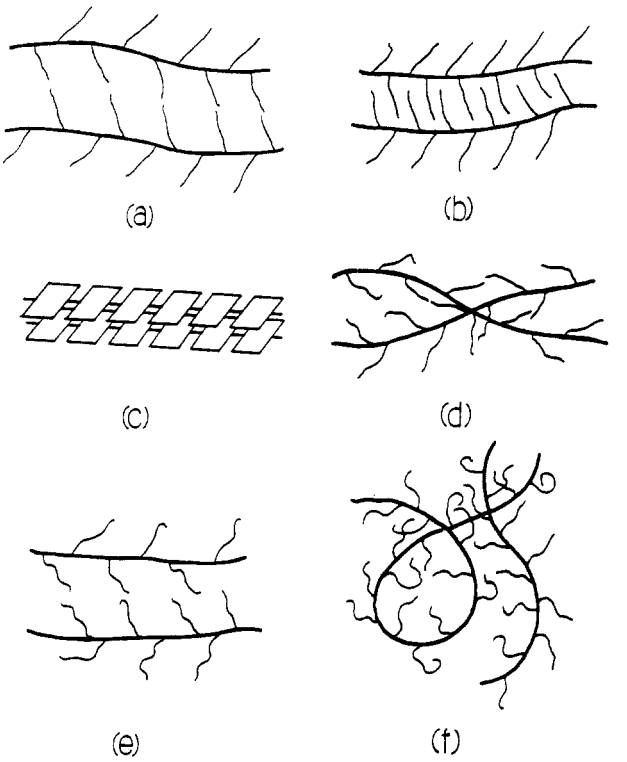

Figure 8. Schematic diagram of the layer structure of a P3AT: (a) ordered two-layer structure, (b) ordered single-layer structure, (c) planar packing, (d) disordered structure before melting (in which a certain degree of chain alignment still is retained), (e) disordered side-chain and ordered main-chain structure, (f) melt structure (in which the conformation of the main chains is random coillike).

Structure of P3ATs and Conclusion

From the experimental results and analysis above, the structure of the P3ATs are proposed as shown in Figure 8. The presence of X-ray diffraction peaks at low angles and the correlation of their corresponding d spacings with the lengths of the side chains in all-trans conformation suggest a two-layer structure and a one-layer structure for the packing of side chains as shown in parts a and b of Figure 8, respectively. That at wide angles giving a d spacing of 3.8 Å for the three P3ATs suggests an intraplanar stacking of the coplanar subchains as shown in Figure 8c. The structures in Figure 8a–c constitute the ordered phase. In the ordered phase, the polymer with the two-layer structure is the majority; these are only small fractions of the one-layer structure. For the disordered phase before melting, the structure as in Figure 8d is suggested for the following reasons: (a) the presence of β and α relaxations of disordered side chains and noncoplanar subchains (from DMA), respectively, and (b) the participation of π-electron delocalization along the chain before the start of the α relaxation process in the disordered subchains (soft conformons) (from UV–vis and DMA). As the temperature rises to the melting range of side chains for P3DDT, the

ordered coplanar subchains still retain good ordering (from DSC) as shown in Figure 8e. As the ordered phase melts, the conjugating length in the main chains is low; the structure of the melt is suggested as shown in Figure 8f. At a temperature before the start of the α relaxation process, the P3ATs are composed of structures a–d. At a temperature above the melting temperature of the side chains, structures a and b are replaced by e. As the temperature rises to above T_m, the whole material is of structure f.

As the side chain is long enough (P3DDT), it can form a separated ordered phase. For all three P3ATs, the disordered phase exhibits γ, β, and α relaxations as in the case of conventional semicrystalline polymers. The γ and β relaxations have a slight contribution to the coplanarity in the main chains. However, the α relaxation has a significant effect on the optical band gap by an increase of the distortion in the soft conformons leading to a localization of their π electrons. At a temperature about 30–60 °C above T_α, the hindered charge transport is dominated over the increased charge mobility, causing the occurrence of a conductivity maximum. This conductivity maximum can be considered as another characteristic of the electronic structure of the π system in addition to thermochromism at T_m.

Acknowledgment. We thank the National Science Council of ROC for financial aid through the project Studies on Soluble Conjugated Conducting Polymers: Structure/Properties and Electrochemical Phenomena, NSC 80-0416-E007-01.

References and Notes

(1) Sato, M.; Tanaka, S.; Kaeriyama, K. *J. Chem. Soc., Chem. Commun.* **1985**, 713.
(2) Jen, K. Y.; Miller, G. G.; Elsenbaumer, R. L. *J. Chem. Soc., Chem. Commun.* **1986**, 1346.
(3) Rughooputh, S. D. D. V.; Nowak, M.; Hotta, S.; Heeger, A. J.; Wudl, F. *Synth. Met.* **1987**, *21*, 41.
(4) Rughooputh, S. D. D. V.; Hotta, S.; Heeger, A. J.; Wudl, F. *J. Polym. Sci., Polym. Phys. Ed.* **1987**, *25*, 1071.
(5) Winokur, M. J.; Spiegel, D.; Kim, Y.; Hotta, S.; Heeger, A. J. *Synth. Met.* **1989**, *28*, c419.
(6) Bolognesi, A.; Catellani, M.; Destri, S. *Makromol. Chem., Rapid Commun.* **1991**, *12*, 9.
(7) Inganäs, O.; Salaneck, W. R.; Österholm, J. E.; Laakso, J. *Synth. Met.* **1988**, *22*, 395.
(8) Inganäs, O.; Gustafsson, G.; Salaneck, W. R.; Österholm, J. E.; Laakso, J. *Synth. Met.* **1988**, *28*, c377.
(9) Salaneck, W. R.; Inganäs, O.; Théman, B.; Nilsson, J. O.; Sjögren, B.; Österholm, J. E.; Brédas, J. L.; Svensson, S. *J. Chem. Phys.* **1988**, *89*, 4613.
(10) Salaneck, W. R.; Inganäs, O.; Nilsson, J. O.; Österholm, J. E.; Thémans, B.; Brédas, J. L. *Synth. Met.* **1989**, *28*, c451.
(11) Thémans, B.; Salaneck, W. R.; Brédas, J. L. *Synth. Met.* **1989**, *28*, c359.
(12) Sugimoto, R.; Taketa, S.; Gu, H. B.; Yoshino, K. *Chem. Press* **1986**, *1*, 635.
(13) Hotta, S.; Hosaka, T.; Soga, M.; Shimotsuma, W. *Synth. Met.* **1984**, *9*, 381.
(14) Rembaum, A. *Encyclopedia of Polymer Science and Technology*; Mark, H., Ed.; John Wiley: New York, 1972; Vol. 11, p 320.
(15) Miller, R. L.; Boyer; R. F. *J. Polym. Sci., Polym. Phys. Ed.* **1984**, *22*, 2021.
(16) Hsieh, H. W. S.; Morawetz, H. *J. Polym. Sci., Polym. Phys. Ed.* **1976**, *14*, 1241.
(17) Plate, N. A.; Shibaev, V. P. *Comb-Shaped Polymers and Liquid Crystals*; Cowie, J. M. G., Ed.; Plenum Press: New York, 1987; p 40.
(18) Gonzalez de la Campa, L. J.; Barrales-Rienda, J. M. *Preprint of short communications of the International Symposium on Macromolecules*; Mainz, West Germany, 1979; Vol. 8, p 1567. Also ref 17, p 62.
(19) Chen, S. A.; Chan, W. C. *J. Polym. Sci., Polym. Phys. Ed.* **1990**, *28*, 1499.
(20) Heijboer, J. *Physics of Non-Crystalline Solids*; Prins, J. A., Ed.; North-Holland: Amsterdam, The Netherlands, 1965; p 231.
(21) Plate, N. A.; Shibaev, V. P. *J. Polym. Sci., Macromol. Rev.* **1974**, *8*, 178.
(22) Chen, S. A.; Li, L. S. *Makromol. Chem., Rapid Commun.* **1983**, *4*, 503.
(23) Chen, S. A.; Li, L. S. *Makromol. Chem.* **1984**, *185*, 1063.
(24) Masuda, T.; Tang, B. Z.; Tanaka, A.; Higashimura, T. *Macromolecules* **1986**, *19*, 1459.
(25) Gibson, H. W. *Handbook of Conducting Polymers*; Skotheim, T. A., Ed.; Marcel Dekker: New York, 1986; Vol. 1, p 428.
(26) Wang, Y.; Rubner, M. F. *Synth. Met.* **1990**, *39*, 153.
(27) Aubrey, D.; Barnatt, A. *J. Polym. Sci., Polym. Phys. Ed.* **1968**, *6*, 241.
(28) Tourillon, G.; Garnier, F. *J. Polym. Sci., Polym. Phys. Ed.* **1984**, *22*, 33. Tourillon, G.; Garnier, F. In *Handbook of Conductive Polymers*; Skotheim, T. A., Ed.; Marcel Dekker: New York, 1986; Vol. 1, pp 307–312.
(29) Yassar, A.; Roncali, J.; Garnier, F. *Macromolecules* **1989**, *22*, 804.
(30) Yoshino, K.; Park, D. H.; Park, B. K.; Onoda, M.; Sugimoto, R. *Jpn. J. Appl. Phys.* **1988**, *27*, L1612.
(31) Paloheimo, J.; Stubb, H.; Yli-LAhti, P.; Kuivalainen, P. *Synth. Met.* **1991**, *41–43*, 563.